

Effect of Dangling Chains on Adhesion Hysteresis of Silicone Elastomers, Probed by JKR Test

Nicolas Amouroux and Liliane Léger*

Laboratoire de Physique de la Matière Condensée, U.M.R. CNRS 7125, Collège de France,
11 Place Marcelin Berthelot, 75231 Paris Cedex 05, France

Received July 29, 2002

The JKR test has been used to quantify adhesion hysteresis between PDMS model networks having different amount of dangling chains. The adhesion hysteresis $G - W$ appears time dependent, and increases with the amount of dangling chains. In accordance with recent investigations of interactions between a brush and an elastomer, it is believed that this hysteresis comes from the progressive bridging of the interface by pendant chains present in the network.

Introduction

When two pieces of elastomers are in contact, the energy required to separate them is often larger than the Dupré's thermodynamic work of adhesion W . The corresponding adhesion hysteresis $G - W$ with G the energy release rate in the separation of the two materials can have different origins. First, real elastomers are not purely elastic, and thus exhibit internal viscous losses when mechanically excited. If the separation is performed at a finite rate, some energy is dissipated at the fracture line. Adhesion hysteresis can also have a chemical origin: during the time of contact some primary or secondary bonds can form. Even if the number of bridges between the two elastomers is small, high energy will be needed to break the interface even at very slow rate, because of the amplification mechanism first described by Lake and Thomas¹ for bulk elastomer fracture and further developed by Gent et al.² for elastomer–elastomer bonding. In the absence of chemical bonding, adhesion hysteresis may come from physical bridging. It is known that elastomers always contain defects such as dangling chains. These chains can act as connector molecules, and lead to an adhesion energy higher than W even at zero rate of separation.^{3,4} The efficiency of connectors molecules to promote adhesion at elastomer interfaces has been investigated by many researchers over the past decade.^{5,6,7} However, these studies were performed with elastomers in contact with a rigid surface grafted with polymer molecules of same nature as the elastomer. Perutz et al.⁸ recently studied elastomer–elastomer contacts, and attributed the observed adhesion hysteresis to the complexation of remaining unreacted cross-linker sites to the catalyst. We present an investigation of the interaction between tailored elastomers made of poly(dimethylsiloxane) (PDMS), and having identical chemistry but different amount of dangling chains. The JKR test is used to probe the adhesion hysteresis, since it gives access to slow rate of crack propagation and offers a high sensitivity to weak adhesion phenomenon.

Table 1. Equivalent Composition of the Elastomers Prepared with Pentamethyldisiloxane (MD')

real system (eq)				equivalent system (eq)				part of sol fraction
r	B_2	D'_4	MD'	r	B_2	$B_1 = B_2 + MD'$	D'_4	$B_2 + 2MD'$
1.2	100	55	20	1.22	80.7	18.6	55	0.7
1.2	100	50	40	1.25	62.8	34.4	50	2.8

Synthesis of Networks with Controlled Structure

The networks were prepared by end-linking of vinyl end-capped PDMS. The polymer was obtained from a commercial PDMS grade (Rhodia Silicone 621V200). The low molecular weight fractions present in the initial commercial broad distribution were taken out by several precipitations in acetone. The final number average molecular weight was $M_n = 16.7$ kg/mol, as deduced from the titration of the vinyl chain ends. Size exclusion chromatography gave a polydispersity index of 1.3, with a somewhat lower value of M_n (15 ± 1 kg/mol) indicating at least 90% of vinyl end capping. The networks were formed by hydrosilylation on 1,3,5,7-tetramethyltetracyclosiloxane using Karstedt's Pt as catalyst (20 ppm). The mixture PDMS/cross-linker was performed at low temperature (-15 °C) in a glovebox under N_2 atmosphere ($RH < 5\%$). Small lenses were then formed by depositing droplets of the unreacted mixture on fluorinated glass plates. Flat ribbons were also prepared using larger quantities of the mixture deposited on the same glass plates, leading to large drops flattened by gravity. At this stage, the samples were taken out of the glovebox and immediately placed in an oven at 100 °C. Networks were cured for 18 h, and then soaked in toluene for 10 days in order to remove the sol fraction. The catalyst was poisoned with 1-dodecanethiol diluted at ~ 300 ppm in the last toluene bath. After extraction, lenses and ribbons were first allowed to dry at room temperature and further placed overnight in an oven at 100 °C in order to remove all toluene. Sol fraction $w_s = (m_0 - m_{\text{extr}})/m_0$ and swell ratio $q_2 = V_{\text{swollen}}/V_{\text{extr}}$ (where m_0 and m_{extr} are the masses of the ribbon prior and after extraction, and V_{swollen} and V_{extr} are the volumes of the swollen and dry extracted networks respectively) were calculated from weight measurements of large pieces of ribbon (initial weight ~ 1 g).

Dynamical mechanical analysis were performed with a RSAII Rheometrics solid analyzer, at 23 °C, with samples of typical dimension 30×10^1 mm³ taken from the extracted ribbons. A weak pretension was applied. The linearity of the mechanical response was checked in the range 0.1 and 2% of tensile deformation. To obtain the best sensitivity a tensile deformation of 2% was used.

Results

Table 2 shows that for the networks prepared with D'_4 and divinyl PDMS the sol fraction w_s is minimal and the swell ratio q_2 becomes maximal for a stoichiometric ratio

- (1) Lake, G. J.; Thomas, A. G. *Proc. R. Soc. A* **1967**, *300*, 108–119.
- (2) Chang, R.-J.; Gent, A. N. *J. Polym. Science* **1981**, *19*, 1619–1633.
- (3) de Gennes, P.-G. *J. Phys. France* **1989**, *50*, 2551–2562.
- (4) Raphaël, E.; de Gennes, P.-G. *J. Phys. Chem.* **1992**, *96*, 4002.
- (5) Creton, C.; Brown, H. R.; Shull, K. R. *Macromolecules* **1994**, *27*, 3174.
- (6) Deruelle, M.; Léger, L.; Tirrell, M. *Macromolecules* **1994**, *28*, 7419.
- (7) Tardivat, C. Ph.D. Thesis, Université Paris XI, 1998.
- (8) Perutz, S.; Kramer, E. J.; Baney, J.; Hui, C.-Y.; Cohen, C. *J. Polym. Sci. Part B: Polym. Phys.* **1998**, *36*, 2129–2139.

Table 2.

system <i>r</i>	measured				calculated				
	<i>q</i> ₂	<i>w</i> _s , %	<i>p</i> _{SiH} , %	<i>p</i> _{C=C} , %	<i>w</i> _e , %	<i>w</i> _p , %	<i>v</i> , mol/m ³	<i>μ</i> , mol/m ³	<i>T</i> _e , %
0.8	8.18	16.45	84.6	67.7	35.35	48.2	11.9	7.45	12
1.0	5.28	5.23	81.3	81.3	59.52	35.25	25.4	15.4	35
1.2	4.10	1.34	76.3	91.5	78.16	20.5	35.8	21.4	61
1.5	3.92	1.18	64.4	96.6	79.42	19.4	30.9	19.0	63
2.0	5.61	3.19	49.0	98.0	67.51	29.3	18.8	11.9	46
1.22 MD'10	4.61	3.0–2.3 ^a	78.2	95.6	67.5	30.2	29.8	18.0	56
1.25 MD'20	5.32	6.5–3.7 ^a	79.2	99.0	53.5	42.8	20.8	12.8	42

^a Corrected by taking into account the chains end capped at both ends by MD' (see text and Table 1).

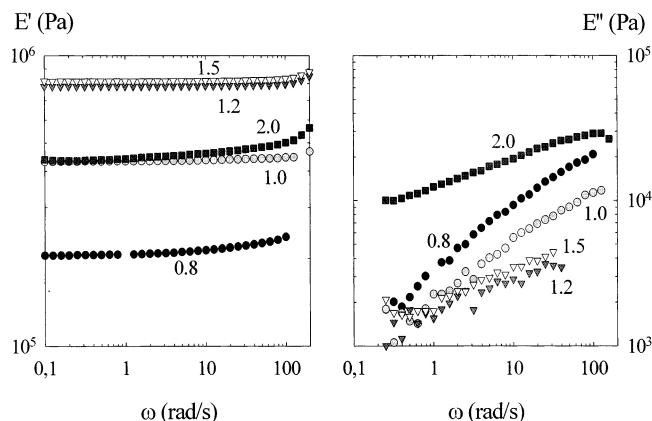


Figure 1. Elastic E' and loss moduli E'' versus pulsation for networks prepared with increasing $r = \text{SiH/C}=\text{C}$ ratio.

$r = \text{SiH/C}=\text{C}$ between 1.2 and 1.5. Examination of Figure 1 also shows that the elastic modulus goes through a maximum and the loss modulus through a minimum for a ratio r between 1.2 and 1.5. Networks corresponding to the ratio $r = 1.2$ seem to be the most “perfect”, and are taken as reference networks.

To obtain networks with a controlled amount of dangling chains but identical chemistry (i.e. same ratio $\text{SiH/C}=\text{C}$), small quantities of pentamethyldisiloxane (MD' in silicone nomenclature: $\text{MD}' = \text{Si}(\text{CH}_3)_3\text{OSi}(\text{CH}_3)_2\text{H}$, molecular mass 0.148 kg/mol) were added in the reaction bath. The unique SiH end of this molecule adds on one vinyl end group of a chain, giving a dangling chain (provided the other chain end is linked to a D'_4). Two networks with 10 and 20 mol % of MD' relative to the quantity of vinyl groups were prepared keeping the overall ratio $\text{SiH/C}=\text{C}$ at 1.2. The effect of MD' addition on the mechanical properties has been investigated by dynamical measurements. Figure 2 shows that the elastic modulus E' is lowered when the network is prepared with MD'. The decay in E' is proportional to the added quantity of MD'. The loss modulus for pulsations higher than 10 rad/s increases with the amount of MD'. The loss moduli increase with frequency and remain very low compared to elastic moduli. The elastic and loss moduli for an elastomer prepared with a $r = 1.0$ but without any MD' are also shown in Figure 2 and are very close to the corresponding moduli for the elastomer with 20% MD' and $r = 1.2$.

Analysis of Network Structure. The necessity to work with a slight excess of SiH to obtain an optimized network may be explained by the fact that the reaction between antagonist groups becomes more and more difficult since reactive species become scarcer, and the network becomes tighter as the reaction progresses. SiH groups are also known to be sensitive to side reactions, particularly with water. Lestel et al.⁹ reported the

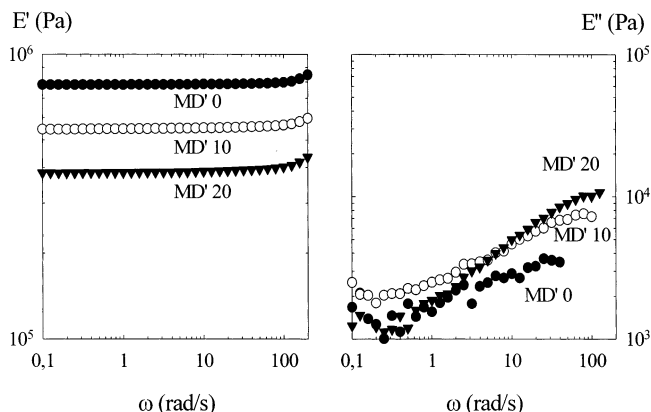


Figure 2. Elastic E' and loss moduli E'' versus pulsation for networks prepared with 0, 10, and 20 mol % of MD' and an overall ratio $\text{SiH/C}=\text{C}$ of 1.2. The moduli for a network prepared without MD' but at a ratio $r = 1$ are also shown for comparison.

following reactions in the presence of Pt catalyst:



The consequence on the network is an increase of the functionality of the cross-links (reaction 2), and a loss of elastically active chains (reaction 3). To minimize these reactions, special care was taken to perform the synthesis in anhydrous conditions as explained before.

Our aim is to estimate the quantity of pendant structures in the network i.e., chains which are connected to the infinite gel by only one end. It is important to notice that a pendant structure can be composed of a number of individual chains. The analysis is based on the recursive method developed by Miller and Macosko¹⁰ and further by Villar, Bibbo, and Vallés.¹¹

The recursive method allows one to compute the theoretical extent of reaction from the sol fraction data. For the sake of simplicity, it is assumed that (i) the chains were functionalized at both ends at the beginning, (ii) the possibility of side reactions (as described above) is neglected, and (iii) the hypothesis of the recursive method itself are correct for our networks.

Once the extent of reaction is known, the concentration in effective junctions μ , the concentration in active junctions ν , the number of trapped entanglement T_e , and the weight fraction of pendant material w_p are readily obtained.

For the network prepared with MD', the evaluation of the network parameters is slightly more complex. How-

(10) Miller, D. R.; Macosko, C. W. *Macromolecules* **1976**, *9*, 206.

(11) Villar, A. M.; Bibbo, M. A.; Vallés, E. M. *Macromolecules* **1996**, *29*, 4072–4080.

(9) Lestel, L.; Cheradame, H.; Boileau, S. *Polymer* **1990**, *31*, 1154.

ever, making the assumption that all the MD' react on vinyl end groups, we can consider that we are dealing with a network made from bifunctionnal B₂ and monofunctionnal B₁ chains, cross-linked by tetrafunctional molecules D'₄, a situation analyzed by Villar et al.¹¹ We however have to take into account the event of chains which react at both ends with MD', and are thus part of sol fraction. The sol fractions were 3.0% and 6.5% for the 10 and 20 mol % networks, respectively. The probability for a chain to have its both ends capped with MD' is given by the square of the MD' mole fraction. For 10 and 20 mol %, 0.7% and 2.8%, respectively, of divinyl chains are thus expected to be part of the sol fraction. The corrected sol fractions are therefore 2.3% and 3.7%, respectively, for these networks. The ratio r has also to be corrected (1.22 and 1.25, respectively). The equivalent systems for networks including MD' end cappers are summarized in Table 1.

The parameters of the networks derived from the recursive method are listed in Table 2. The extent of reaction for SiH and C=C varies in reverse order as r increases. The ratio $r = 1.2$ combines a good extent of reaction for both species. For this ratio, the concentration in elastically active chains ν , and active knots μ are correspondingly the highest.

The fraction of pendant structure w_p is always larger than ~20%. When one adds MD', the fraction of dangling chains increases quite linearly as expected. Unlike networks prepared at $r = 0.8$ or $r = 1.0$, which have quite similar amounts of dangling chains, the extent of reaction of SiH and C=C is as large as that for the network prepared at $r = 1.2$ without MD', and the sol fraction is low.

Consistency of Molecular Structure with Mechanical Properties. To check the consistency of the results obtained with the recursive method, we tried to correlate them with the mechanical analysis. The elastic Young modulus can be computed from the molecular parameters as follows:¹²

$$E = 3(\nu - \mu)RT + 3T_e G_N^0 \quad (1)$$

where R is the perfect gas constant, T the absolute temperature (300 K), and G_N^0 the plateau shear modulus (between 0.2 and 0.3 MPa for PDMS¹³). The first term is given by the phantom network theory, and the second one is the contribution of the trapped entanglements.

The elastic modulus can be deduced from the swelling data:

$$E = 3\nu_{FR}RT \quad (2)$$

where ν_{FR} is the concentration in effective elastic chains given the Flory–Rehner relationship:

$$\nu_{FR} = \frac{\ln(1 - \nu_2) + \chi\nu_2^2 + \nu_2}{V_1 \left(\frac{2}{f} \nu_2 - \nu_2^{1/3} \right)} \quad (3)$$

In this equation, $\nu_2 = 1/q_2$ is the fraction of polymer in the swollen network, χ is the Flory interaction parameter ($\chi = 0.415 + 0.427\nu_2$ for PDMS/toluene¹⁴), $f = 4$ the functionality of the cross-linker, and V_1 the volume of a solvent molecule.

Figure 3 shows that the moduli E' and $3\nu_{FR}RT$ are very close and in good agreement with the modulus computed

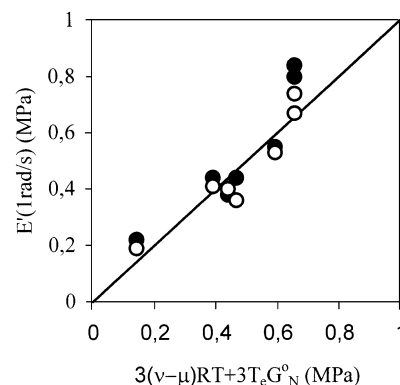


Figure 3. Comparison of the Young modulus obtained from mechanical data (Figures 1 and 2, ●), swelling data (Table 2 and eqs 2 and 3, ○) and the modulus computed from the molecular parameters (Table 2) of the networks using eq 1.

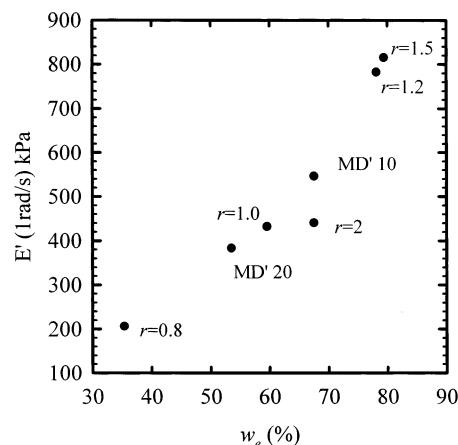


Figure 4. Correlation between the Young modulus obtained from mechanical data (Figures 1 and 2) and the proportion of elastic chains w_e (Table 2).

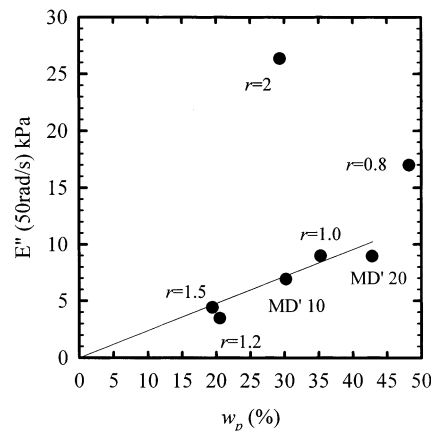


Figure 5. Correlation between the loss modulus E'' obtained from mechanical data (Figures 1 and 2) and the proportion of pendant chains w_p (Table 2).

from the molecular parameters with $G_N^0 = 0.3$ MPa. However, a large part of the computed modulus comes from the entanglement contribution T_e , which is a parameter whose derivation from the recursive method is not really convincing. Alternatively E' correlates very well with the proportion of elastic chains w_e as shown in Figure 4.

It is well-known that dangling chains increase the viscous loss of networks. Figure 5 shows indeed a good correlation between the loss modulus E'' and the fraction of pendant chains, except for networks prepared far from

(12) Langley, N. R. *Macromolecules* **1968**, *1*, 348.

(13) Valles, E. M.; Macosko, C. W. *Macromolecules* **1978**, *12*, 4, 673.

(14) Gottlieb, M.; Herskowitz, M. *Macromolecules* **1981**, *14*, 1468.

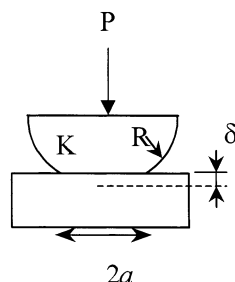


Figure 6. JKR geometry. P is the applied force, a radius of the contact area, δ is the sum of the displacements of the lens and ribbon surface, K is the rigidity constant of the system, and R the radius of curvature of the spherical lens.

stoichiometry at $r = 2.0$ or $r = 0.8$. For these networks, due to a large off-stoichiometry, the pendant structures should be tree like, of high molecular weight, and thus very dissipative.

Conclusion

The addition of MD' end cappers gives networks with optimized chemistry and adjustable content of dangling chains. The analysis of the network with the recursive method seems to indicate that the hydrosilylation was not completed. However, some of the residual groups should have reacted with water traces, due to side reactions, giving knots with higher functionality or dangling chains. Despite such side effects were not taken into account in the analysis, the molecular parameters obtained are qualitatively consistent with the mechanical properties of the networks. The three networks prepared at $r = 1.2$ with 0, 10, and 20 mol % of MD' are very close in chemistry, but exhibit increasing amount of dangling chains. These networks, after extraction and neutralization of the Pt catalyst, have been used for the characterization of their adhesion behavior by JKR test.

Adhesion Results

JKR Theory. The JKR test derived from the theory of Johnson, Kendall, and Roberts¹⁵ has been extensively used these last years for the investigation of the adherence of soft elastomers on various substrates.^{6,16,17} The geometry is a sphere-plane as shown in Figure 6. The sphere is characterized by an elastic modulus K_1 and a radius of curvature R_1 . In the present paper, the other body will be a flat ribbon ($R_2 = \infty$) of the same elastomer as the lens ($K_2 = K_1$). In the present case the system is defined by an equivalent radius of curvature $R = R_1$ and an equivalent modulus $K = K_1/2$:

$$R^{-1} = R_1^{-1} + R_2^{-1} = R_1^{-1}$$

$$K^{-1} = K_1^{-1} + K_2^{-1} = \frac{3(1 - \nu_1^2)}{4E_1} + \frac{3(1 - \nu_2^2)}{4E_2} = 2K_1^{-1} = \frac{9}{8E} \quad (4)$$

where ν_i and E_i are respectively the Poisson coefficient ($\nu = 1/2$ for incompressible elastomer) and the Young modulus of each material, in the general case.

The elastic spherical lens is submitted to a loading-unloading cycle against the flat elastomer. The contact

may be described by three observables: the deformation δ of the system, the contact radius a , and the applied force P . From the evolution of these observables during one cycle, one obtains an energy release rate G :

$$G = \frac{\left(\frac{Ka^3}{R} - P\right)^2}{6\pi Ka^3} \quad (5)$$

For perfectly reversible contacts and for quasistatic loading/unloading rates, G is equal to the thermodynamic work of adhesion of Dupré W . The inverted form of eq 5 is known as the JKR equation:

$$a^3 = \frac{R}{K} [P + 3\pi GR + \sqrt{6\pi GRP + (3\pi GR)^2}] \quad (6)$$

The JKR theory imposes the following relationship between δ and P , which is independent of G :

$$\delta = \frac{a^2}{3R} + \frac{2P}{3aK} \quad (7)$$

JKR theory holds for semiinfinite medium. For JKR studies using large moulded spheres this condition is easily fulfilled. On the other hand, the use of small lenses offers considerable advantages. Small lenses can easily be made as explain before. Moreover, small lenses have a large surface volume ratio which gives a high sensitivity to surface interactions. Indeed, in the particular case of zero force the JKR theory holds:

$$\frac{a_0}{R} \propto \left(\frac{G}{R}\right)^{1/3} \quad (8)$$

where a_0 is the contact radius at zero force and R the radius of curvature of the sphere. The smaller is R , the higher is the a_0 over R ratio for a given G .

On the other hand, lenses of millimeter size obviously do not fulfill the assumption of infinite medium of the JKR theory. One observes a departure from the law $\delta(a, P)$ which disappears when the height of the lens is larger.¹⁸ On the contrary, the effect of the thickness of the lens on the law $a^3(P)$ is negligible. In fact, it can be shown^{19,20} that the stress within the lens varies inversely to the square of the distance z from the contact plane ($1/z^2$), whereas the displacement decays inversely to the distance ($1/z$). Therefore, for lens thickness h such that $a/h < 0.1$, the JKR laws $G(a, P)$ and $a^3(P)$ are correct, and the $\delta(a, P)$ is corrected as follows:

$$\delta = \delta_{\text{JKR}} - \frac{\beta}{Kh} P \quad (9)$$

where β is a constant equal to $8/3\pi^{19}$ or $2/3$.²¹

JKR Setup. The homemade JKR setup consists essentially of a motorized vertical stage under which the lens is placed. The flat elastomer is placed on the plateau of a force sensor of stiffness $k = 256$ N/m under the stage. An optical setup comprising a CCD camera and a Questar microscope coupled to a video frame grabber allows the automatic measurement of the radius of the contact area,

(18) Deruelle, M.; Hervet, H.; Jandeanu, G.; Léger, L. *J. Adhes. Sci. Technol.* **1998**, 12-2, 225-247.

(19) Amouroux, N. Ph.D. Thesis, Université Paris VI, 1998.

(20) Hui, C. Y.; Lin, Y. Y.; Baney, J. M.; Jagota, A. *J. Adhes. Sci. Technol.* **2000**, 14-10, 1297-1319.

(21) Shull, K. R.; Anh, D.; Chen, W. L.; Flannigan, C. M.; Crosby, A. J. *Macromol. Chem. Phys.* **1998**, 199.

(15) Johnson, K. L.; Kendall, K.; Roberts, A. D. *Proc. R. Soc. A* **1971**, 324, 3001-313.

(16) Chaudhury, M. K.; Whitesides, G. M. *Langmuir* **1991**, 7, 1013.

(17) Anh, D.; Shull, K. R. *Macromolecules* **1996**, 29, 4381.

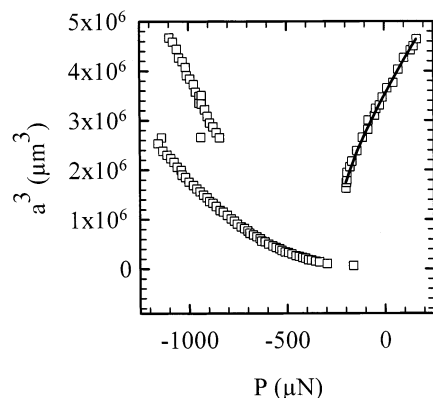


Figure 7. Typical JKR experiment for a network at 20% MD' against itself, illustrated in the (a^3, P) plane. The line corresponds to the best fit of the loading data with eq 6 which gives $K = 0.36$ MPa and $W = 42$ mJ/m² for this experiment. After a contact time of nearly 4 h, the unloading is performed, in two steps in this example. The G values are obtained by eq 5 from the unloading (a^3, P) points and V is obtained through discrete derivation of a with respect to time.

a (three measurements per second). The stage displacement Δ , force P , and radius of contact a are monitored as a function of time. The stage displacement Δ is measured by a LVDT sensor. The real displacement δ can be deduced from Δ since $\Delta = \delta_{\text{offset}} + \delta + P/k$.

The radius R and the height h of each lens were measured from side-views under microscope. The typical thickness of the flat ribbon was 1 mm, and the height of the lens 0.7 mm. To limit finite size effects a ribbon was placed under the lens to increase the effective thickness of the lens up to 1.7 mm.

A typical experiment comprises¹⁸

1. a step-by-step loading of the system by small increase of Δ (0.5 μm) each 30s, up to a given contact radius (100–150 μm). The adjustment of the experimental $a^3(P)$ curve to eq 6 gives K and W ;

2. a chosen time of rest under load during which interactions at the interface may develop (from minutes to days);

3. an unloading: Δ is decreased suddenly by $\sim 5 \mu\text{m}$, and $a(t)$ and $P(t)$ are then recorded while Δ stays constant. This sequence is repeated until the contact breaks off. The energy release rate G is computed from a versus P data, injecting in eq 5 the value of the modulus K obtained through the loading experiment, and the velocity of the crack tip $V = -da/dt$ is obtained by discrete derivation of a as a function of time. A $G(V)$ unloading curve is thus obtained.

These three steps are illustrated in Figure 7.

JKR Results. From loading data a value of W in the range 40–45 mJ/m² is obtained for all the elastomers. This value is, as expected, close to twice the surface energy for PDMS ($\gamma = 21.6$ mJ/m²). The rigidity constants K for the different elastomers were also given by the loading data and were compatible with the results for the elastic moduli E at low pulsations shown in Figure 2.

The $G(V)$ curves given by the unloading data were found to depend on the contact time as shown in Figure 8 for networks with 10% MD'. For short contact times, no adhesion hysteresis is visible: the values of G at low velocities are very close to W . As the contact time increases, $G(V)$ shifts to higher values. Since it is not easy to extrapolate G at zero crack velocity, we compare the evolution with time of the adhesion hysteresis $G-W$ at a low crack velocity (0.1 $\mu\text{m/s}$) for the three networks (Figure 9). It is apparent that the level of adhesion hysteresis

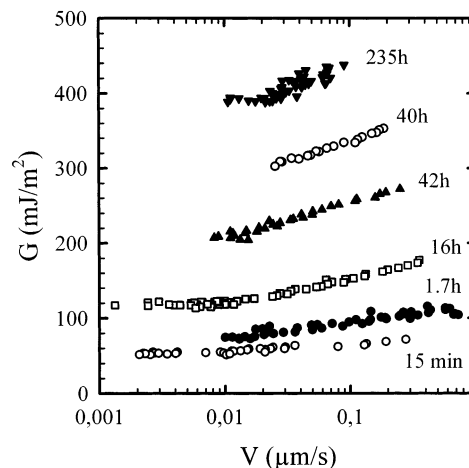


Figure 8. Elastomer $r = 1.2$ with 10 mol % MD': $G(V)$ curves obtained from unloading data for increasing contact times, as indicated.

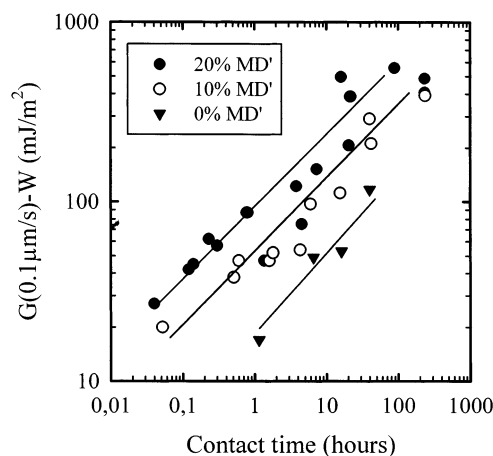


Figure 9. Plot of the adhesion hysteresis $G - W$ at finite velocity 0.1 $\mu\text{m/s}$ versus the contact time in log–log scale. The lines are only guides for the eyes.

increases in a similar way for all networks. A fit with a power law would give an exponent of ~ 0.4 ; however, the scatter in the data does not allow a more accurate description of the kinetics. For the elastomer MD'20, it seems that a plateau value of ~ 500 mJ/m² is obtained after at least 1 day of contact. The plateau values for the hysteresis would be in the vicinity of ~ 300 mJ/m² for MD'10 and ~ 100 mJ/m² for MD'0. At all times of contact, it is apparent that the hysteresis depends on the amount of pendant chain in the networks.

Discussion

Adhesion hysteresis may arise from different sources. Material viscoelasticity can be the cause of an *apparent* adhesion hysteresis. At very low velocity, dissipation in the material close to the crack tip should be negligible and the value of the intrinsic adhesion energy G_0 obtained. At a finite velocity the value of G is indeed enhanced with the increase of the dissipative character of the material at a given G_0 . These viscoelastic effects can be taken into account if one introduces a dissipative function. Following Maugis and Barquins²² we have

$$G = G_0(1 + \phi(V)) \quad (10)$$

This equation shows that the adhesion hysteresis at a given velocity $G(V) - W$ can be much higher than the real

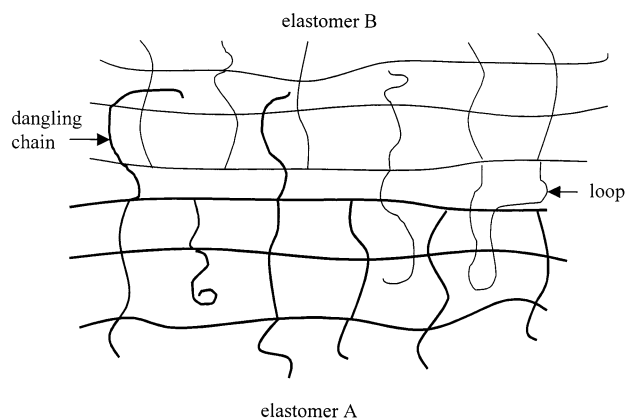


Figure 10. Schematics of the interface between the two elastomers. Interdigitation occurs through dangling chains or loops.

adhesion hysteresis $G_0 - W$ if $\phi(V)$ is not negligible compared to 1. In cases where G_0 reduces to W , one can believe wrongly, with data taken at a given velocity, that there is an adhesion hysteresis. In the data presented here, it is apparent that viscoelastic effects are present at least above $0.01 \mu\text{m/s}$ even if our materials have small loss moduli.

In the present case viscoelastic effects are not the only origin of the adhesion hysteresis since we observe an increase of G with contact times. Perutz et al.⁸ attributed adhesion hysteresis for PDMS elastomers to complexation of remaining SiH groups with the Pt complex, for elastomers prepared with an excess of cross-linker. However in our system, all elastomers are prepared with the same stoichiometric ratio, the catalyst is poisoned and the networks are extracted. Therefore complexation does not explain our experiments.

The various networks we have tested differ by the amount of dangling chains. A dangling chain close to the surface of one elastomer can diffuse in the other elastomer when an intimate contact is formed between both elastomers. This situation is illustrated in Figure 10. This process is time dependent. When the two elastomers are pulled apart, the bridging chains must be extracted from the elastomers. It has been shown⁴ that a minimal force is required for a "molecular fibril" to exist even at zero velocity, resulting in a value of the adhesion energy G_0 higher than W . This value is predicted to be linearly dependent on the polymerization index N and the areal

density Σ of the bridging molecules:

$$G_0 - W \propto \gamma \Sigma N \quad (11)$$

For a system involving a brush and an elastomer, this equation does not hold for high areal density since the penetration of the connector molecules is prevented by the finite elasticity of the network. In the case of contact between elastomers, this limiting elastic effect should be avoided, since the same amount of dangling chains is exchanged from both sides (for symmetric systems).

The adhesion hysteresis observed in our experiments may thus arise from interdiffusion of chains across the interface as sketched in Figure 10. The values obtain for G are in the same range of values obtained for systems involving a PDMS grafted layer and a PDMS elastomer.⁷ The very long times observed in our system may be related to the fact that the pendant material in the networks has certainly a branched structure leading to long relaxation times. Such long times were also encountered for polyisoprene elastomer/polyisoprene brush systems (H. R. Brown⁵) and PDMS elastomer/PDMS brush systems (Tardivat⁷). The interdigitation kinetics has been analyzed theoretically by Connor and Mac Leish²³ and was found to involve a two steps process. First the free end of the tethered chain has to enter the other network at a point which may be far from its tethered end, next the chain has to find its equilibrium configuration in the network. The branched structure of the pending material involved in the interdigitation process of the present experiments provides additional obvious reasons for a very long relaxation.

Conclusion

Adhesion hysteresis between PDMS elastomers was observed using the JKR test on model networks with different amount of dangling chains. The hysteresis $G - W$ is observed to be time dependent, and to increase with the amount of dangling chains. In accordance with recent studies of interaction between a layer of chains end grafted on a solid surface and an elastomer, it is believed that this hysteresis comes from the progressive bridging of the interface by pendant chains present in the network. The slow kinetics of this process may be related to the branched structure of the dangling material, and not to a repelling effect of the elastomer contrary to what happens in experiments where an elastomer is put into contact with a grafted brush, due to the symmetry of the interdiffusing interfaces.

LA020680E

(22) Maugis, D.; Barquins, M. *J Phys D.: Appl. Phys.* **1978**, *11*, 1989–2023.

(23) O'Connor, K. P.; McLeish, T. C. B. *Macromolecules* **1993**, *26*, 7322.